

Application of green-emitting ZnS:Eu²⁺ for boosting the spectrum of white light-emitting diode packages

Dieu An Nguyen Thi¹, Phuc Dang Huu²

¹Faculty of Electrical Engineering Technology, Industrial University of Ho Chi Minh City, Ho Chi Minh City, Vietnam

²Institute of Applied Technology, Thu Dau Mot University, Thu Dau Mot city, Vietnam

Article Info

Article history:

Received Aug 5, 2021

Revised Apr 16, 2022

Accepted May 11, 2022

Keywords:

Color homogeneity

Color rendering index

Luminous flux

Monte Carlo theory

White light emitting diodes

ABSTRACT

Through utilizing a nonlinear application to acquire the best lumen efficiency (LE) for radiation (also known as LER) when color rendering index (CRI) value, especially CRI of R9 for strong red exceeds 90 with correlated color temperature (CCT) range of 2700-6500 K, the white light emitting diodes (WLED) package with adjustable CCT value and comprised of mixed-type light-emitting diodes (LEDs) can be acquired. The WLED model here contains blue and red LEDs with direct emission and a phosphor-conversion blue LED or pc/B-LED (including orange and green phosphors mixed with blue LED colorant). The peak wavelengths of each LED constituent are 465 and 628 nm for LEDs in blue and red, 452 nm for the blue LED colorant, 530 and 586 nm for the phosphors exhibiting green and orange colors. Under the CCT of 2722-6464 K, the attained actual LED package, either with conversion phosphor, in red or in blue, possibly displays both CRI and R9 values measured from 90 to 96, color quality scale (CQS) values measured from 89 to 94, with LERs and LEs of 303-358 lm/W and 105-119 lm/W, respectively.

This is an open access article under the [CC BY-SA](https://creativecommons.org/licenses/by-sa/4.0/) license.



Corresponding Author:

Phuc Dang Huu

Institute of Applied Technology, Thu Dau Mot University

No 6, Tran Van On Street, Thu Dau Mot city, Binh Duong province, Vietnam

Email: danghuuphuc@tdmu.edu.vn

1. INTRODUCTION

According to certain researches, a novel form of retinal cells that can assess illumination and the ganglion cells can interact with biological clock in our brain through signals [1], [2]. It was demonstrated that under unsuitable illuminated environments, the inner workings of mammals' bodies can be disrupted and create detrimental results in their well-being, such as cancer [3]. As such, utilizing adjustable chromatic temperature in illuminations could improve our physical condition. In addition, this could diminish the need for medicines intended for alleviating sleep deprivation. As such, illuminations that imitate the significant chromatic temperature found in the noon sun, as well as the small chromatic temperatures found in the morning time and nighttime, can be a suitable choice, as our bodies have long become accustomed to these biological illuminations.

There is another option that involves controlling said biological clock. When the biological illuminations can alleviate the tiredness of the people in traffic, it could lead to fewer fatal vehicular incidents [4]. There are certain difficulties in creating the white light emitting diodes (WLED) packages that possess adjustable correlated color temperature (CCT) values, which require us to simultaneously obtain outstanding color rendering index (CRI) output [5] under various CCT levels and produce the best lumen efficiency (LE) values. Researches have examined certain WLED packages mentioned above [6]–[10]. Researches proved that the NW/R/B package containing red and blue light-emitting diodes (LEDs) (with

wavelengths of 631.9 and 463 nm respectively) and the Northwest LED (NW LED) having *Commission Internationale de l'Eclairage* (CIE) 1931 color coordinates of (0.3718, 0.4485) can be the easiest way to acquire significant CRI and LE values. The color position in the NW LED appears to exceed the Planckian locus within the yellow-green zone, while the American National Standards Institute (ANSI) standard in WLED (ANSI C78.377) does not apply to the NW LED. The NW/R/B package, therefore, can produce a three-angle chromatic scale surrounding the Planckian locus and as such, we can adjust the CCT values. Researches have the NW/R/B package having a CRI value over 85, while the special CRI of R9 for strong red scored under 70 [8]. CRI has a downside: it positively evaluates illuminations that display inferior chromatic performance in certain entities under saturated conditions [11], [12]. Specific research [13] points out certain issues in CRI utilized for WLED illuminations. The assessment based on CRI will not properly reflect the optical performance under various circumstances. Among the causes for this, it could be that the distinctive arrangement of the degree in chromatic variance happens when the WLED lights up objects acting as reflectors, caused by the unusual allocations of spectrum energy in the WLED illuminations that influences the reflection of spectrum in the objects used for chroma testing. Notably, such event can be seen in the object number 9 utilized under the CIE technique: a strong red object used for chroma testing.

The National Institute of Standards and Technology has come up with utilizing a better parameter, which is color quality scale (CQS) [14]. Researches proved that the parameter gives evaluations similar to that of CRI in the newest LED devices based on phosphor, red, blue, green, amber (RGBA) LED devices as well as conventional discharge lamps [14]. If considered a mean to assess the performance of chromatic generation in white illuminations, CRI can be used for WLED packages based on conversion phosphor. Researches have examined certain ways to boost the spectrum in WLED devices with non-adjustable CCT value [15]–[22]. On the other hand, no research has aimed at boosting the spectrum in WLED packages with adjustable CCT value. For our research, in order to create a PC/R/B LED package with adjustable CCT, significant LER and CRI values that contains blue and red LEDs with direct emission and LEDs based on conversion phosphor made of orange and green phosphors mixed with blue LED colorant; we utilized a nonlinear application to acquire the best LER value with CRI and R9 values exceeding 90 under the CCT levels in the range of 2700–6500 K with color distinction from the Planckian or daylight locus on the CIE 1960 uv color diagram (dC) under 0.0054.

We examine the special CRI of R9 for strong red as the distinction between red and green could be vital when it comes to chromatic generation, while red can cause issues. An insufficient proportion of red elements can limit the regeneratable chromatic scale and the lightened environment could become visually bland [23], [24]. For our research, we created a PC/R/B package having significant lumen efficiency and performance of chromatic generation. The research also demonstrates the influence from the peak wavelength's inconsistencies in the blue LED colorant, the red and blue LEDs in the said package.

2. RESEARCH METHOD

2.1. Preparation of green-emitting ZnS:Eu²⁺ phosphor

The preparation process of the ZnS:Eu²⁺ phosphor begins with mixing the ingredients by slurring them in water or methanol. Let the mixture dry and pulverize the mixture. Next, add approximately 2 to 3 grams of sulfur. The mixture then goes through two heating stages. In the first stage, heat the mixture in open quartz boats in H₂S at the temperature of 1100 °C for an hour, then pulverize the mixture. In the second stage, heat the mixture in open quartz boats in H₂S at the same temperature for an hour. The resulting phosphor emits yellow-green light; has an emission peak at 2.25 eV, weaker band at 1.95 eV, emission width (FWHM) of 0.24 eV, excitation efficiency by UV as +(4.88 eV), +(3.40 eV) and poor excitation efficiency by e-beam, see Table 1.

Table 1. The composition of ZnS:Eu²⁺

Ingredient	Mole %	By weight (g)
ZnS	100	98
Eu ₂ O ₃	0.03 (of Eu)	0.053

2.2. Spectra optimization of the WLED package with adjustable CCT

Using the LightTools 9.0 application and the Monte Carlo technique, we recreated the layer of phosphor in the multi-chip white LED (MCW-LEDs) having flat layers of silicone. The recreation procedure involves two primary stages. First, we must determine and build the configuration samples and light attributes in MCW-LED lamps. Second, we manipulate the phosphor compounding the impacts of light

through different ZnS:Eu²⁺ concentrations. To assess how the YAG:Ce³⁺ and ZnS:Eu²⁺ phosphor compounding can affect the output of MCW-LED lamps, it is necessary for us to draw several comparisons in connection with the change of the ZnS:Eu³⁺ concentration. The illustration of the WLED simulation is exhibited in Figure 1. Particularly, in Figure 1(a), we can see the overview of the WLED model used for simulation and measurements. Additionally, this WLED model is precisely created to be identical to the real WLED package that possesses optimal thermal stability. The normalized cross correlations of the simulated and the actual WLED models are about 99.6%, which indicates the desired identity between them. Moreover, by recreating the WLED structure that is close to the real one, it contributes to reducing the effects of other lighting features on the CRI and CCT, including LED wavelength, waveform, illumination intensity, and operating temperature. Note that the re-fabricated W-LED lamp has conformal phosphor compounding at a high CCT level measured at 8500 K, meaning that the facets of MCW-LEDs' recreation do not involve ZnS:Eu²⁺. As can be seen in Figures 1(b)-(d), the details of WLED simulation include the reflectors, the chip and the phosphor layers. The reflector's bottom length, height and top surface length are respectively measured at 8, 2.07 and 9.85 mm. The conformal phosphor compounding is coated on the nine chips, each of which has a default 0.08-mm thickness. Every square chip is 1.14 mm long and 0.15 mm tall, and is linked to the gap of the reflector. In every chip, the radiant flux is 1.16 W with the peak wavelength of 453 nm. Besides, more specifications of the WLED simulation are presented in Table 2.

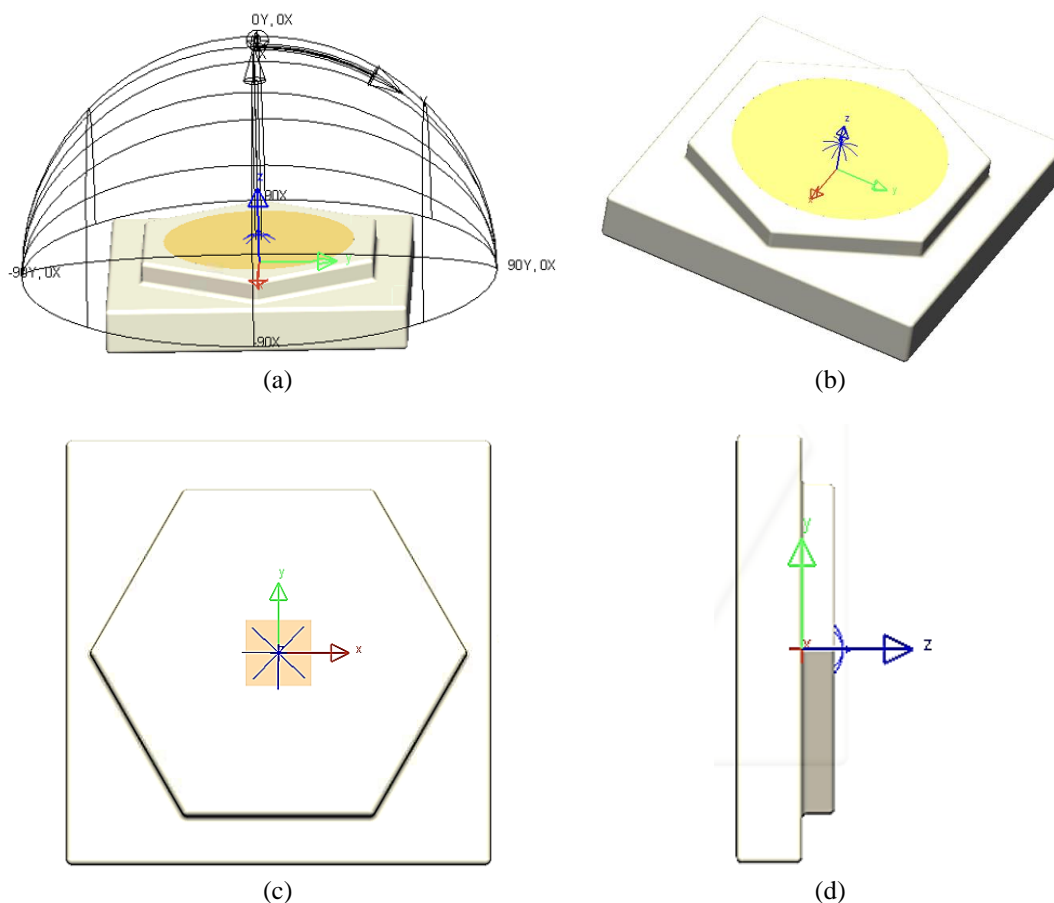


Figure 1. Photograph of WLEDs (a) overview of the simulation and measurement model, (b) detailed simulation LED model, (c) bonding diagram, and (d) side-view illustration of the model

Table 2. Specifications of LED simulation

LED vender	Epistar
LED chip	V45H
Voltage (V)	3.5~3.6
Peak wavelength	453
Power (mV)	320~340
Leadframe	4.7 mm Jentech Size-S
Die attach	Sumitomo 1295SA

After recreating the WLED, the model of expressions to examine the spectra is built, which can be described. The PC/R/B LED package with adjustable CCT contains the LED based on conversion phosphor and blue LED colorant, phosphors in green and orange colors, as well as red and blue LEDs with direct emission. The equation (1) determines the spectral power distribution (SPD) value in the package, represented by $S_{PC/R/B}(\lambda)$ [25]:

$$S_{PC/R/B}(\lambda) = k_{PC}S_{PC}(\lambda, \lambda_b, \lambda_g, \lambda_{or}) + k_R S_R(\lambda, \lambda_R) + k_B S_B(\lambda, \lambda_B) \quad (1)$$

In (1), $S_{PC}(\lambda, \lambda_b, \lambda_g, \lambda_{or})$, $S_R(\lambda, \lambda_R)$, $S_B(\lambda, \lambda_B)$ represents the spectrum in the LED based on conversion phosphor, the red LED and the blue LED; $\lambda_b, \lambda_g, \lambda_{or}, \lambda_R$ represents the peak wavelengths for the blue LED dye, the phosphors in green and orange, the red LED and the blue LED; k_{PC}, k_R, k_B represents the relative SPD's fractions in the conversion-phosphor LED, the red LED and the blue LED. The (2) determines $S_{PC}(\lambda, \lambda_b, \lambda_g, \lambda_{or})$, which represents the relative SPD value for the conversion-phosphor LED:

$$S_{PC}(\lambda, \lambda_b, \lambda_g, \lambda_{or}) = q_b S_b(\lambda, \lambda_b) + q_g S_g(\lambda, \lambda_g) + q_{or} S_{or}(\lambda, \lambda_{or}) \quad (2)$$

In (2), $S_b(\lambda, \lambda_b)$ represents the relative SPD for the blue spectra propagated through the phosphors; $S_g(\lambda, \lambda_g)$ and $S_{or}(\lambda, \lambda_y)$ represents the relative emission spectrum for the phosphors in green and orange; $q_b, q_g,$ and q_{or} represents the fractions of relative emission spectrum for phosphors in green and orange.

With an SPD composed of the emission spectra of blue InGaN and red AlGaInP LEDs along with conversion-phosphor LED having blue InGaN colorant, silicate phosphors in green and orange in the PC/R/B package, this research utilizes the He-Zheng SPDs model [7] in the red AlGaInP LED, blue InGaN LED and silicate phosphors. With photon energy linewidths for the blue InGaN LED and the red AlGaInP LED measured at approximately 5 kT and 2kT, we presume that the half-spectral-width (HSW) values [7] for $S_B(\lambda, \lambda_B)$ and $S_R(\lambda, \lambda_R)$ are 28 and 20 nm. We presume the HSW value for $S_b(\lambda, \lambda_b)$ to be 32 nm, which is attributed to the widening blue spectrum propagated through the phosphors. When it comes to enhancing spectrum, our belief is that the peak wavelength and the HSW in LED are not related to the drive current. As such, $S_{PC/R/B}(\lambda)$ conforms to the linear amalgam of $S_{PC/R/B}(\lambda)$, $S_R(\lambda, \lambda_R)$, $S_B(\lambda, \lambda_B)$ with the fractional factors k_{PC}, k_R, k_B . Similarly, $S_{PC}(\lambda, \lambda_b, \lambda_g, \lambda_{or})$ conforms to the linear amalgam of $S_b(\lambda, \lambda_b)$, $S_g(\lambda, \lambda_g)$, $S_{or}(\lambda, \lambda_y)$ with the fractional factors q_b, q_g, q_{or} . For the process of creating the PC/R/B package, it is necessary to examine the nonlinear aspect and the drive current.

Putting the eleven-dimension parameter space through the chroma-blending limitations will yield the position of the possible vectors over the hyperspace possessing eight dimensions [25]. The formula demonstrated below is intended for enhancing the spectrum in PC/R/B LED package with adjustable CCT:

$$F(\lambda_b, \lambda_g, \lambda_{or}, \lambda_R, \lambda_B, q_b, q_g, q_{or}) = \sum_{i=1}^8 LER_i \quad (i = 1, 2, 3, \dots, 8) \quad (3)$$

(with $CRI_i \geq 90, R_9 \geq 90, dC \leq 0.0054$)

In (3), i is equal to values from 1 to 8 that represent the CCT levels of 2700 K, 3000 K, 3500 K, 4000 K, 4500 K, 5000 K, 5700 K, 6500 K in the PC/R/B package.

3. RESULTS AND DISCUSSION

Figure 2 shows that the green phosphor ZnS:Eu²⁺ concentration is inversely proportional to the yellow phosphor YAG:Ce³⁺ concentration, which indicates two things: first, to maintain the average CCT levels; second, to affect the absorption and scattering WLEDs' two layers of phosphor. The WLEDs' chromatic performance and lumen output can be affected in the end as a result. Therefore, the choice of ZnS:Eu²⁺ concentration determines the WLEDs' chromatic performance. As the said concentration raises from 2% to 20% Wt., the concentration of YAG:Ce³⁺ went down to maintain the average CCT levels. Such event also applies to WLEDs in the CCT range of 5600 K to 8500 K.

Figure 3 demonstrates how the concentration of green phosphor ZnS:Eu²⁺ can influence the WLEDs' transmittance spectrum. The needs of the manufacturer can determine the option. WLEDs with a significant requirement of chromatic performance may slightly decrease the lumen output. As we can see in Figure 3, the combination of the spectral zone creates white light. The said figures display the spectrum at respective CCT levels of 5600 K, 6600 K, 7000 K and 8500 K. It is clear that the two zones of the optical spectrum with the wavelength range of 420 to 480 nm and 500 to 640 nm indicate that their intensities rise accordingly to the concentration of ZnS:Eu²⁺. Such rise in the two-band emission spectrum indicates higher

lumen. In addition, the scattering of blue light in WLED also displays higher activity, indicating higher activity of the scattering in the layer of phosphor and in WLED, which boosts the chromatic homogeneity as a result. Such outcome can be vital for the use of ZnS:Eu²⁺. Specifically, manipulating the chromatic homogeneity in remote phosphor package at great temperature is not easy work. Our research verified the ability of ZnS:Eu²⁺ at small and great color temperatures (5600 and 8500 K) to boost the WLEDs' chromatic performance.

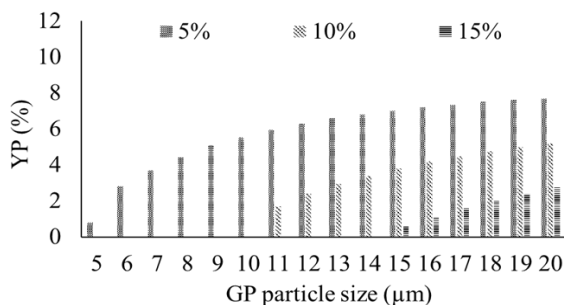


Figure 2. Changing the concentration of phosphorus to preserve the average CCT

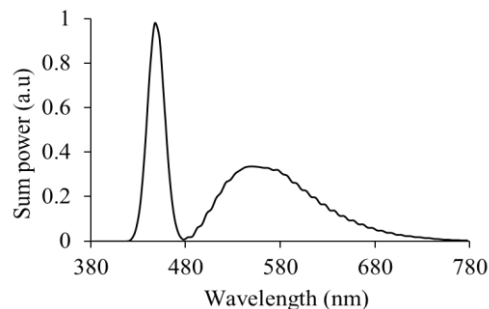


Figure 3. The emission spectra of 8000 K WLEDs as a function of ZnS:Eu²⁺ concentration

This article, therefore, has demonstrated the lumen efficiency in the two-layer remote phosphor layer. Specifically, in Figure 4, the lumen generated is seen to receive a substantial boost as the ZnS:Eu²⁺ concentration goes from 2% to 20% wt. Figure 5 shows that the color deviation displayed a considerable decrease in accordance with the concentration of phosphor ZnS:Eu²⁺ at three average CCT levels. Such event can be clarified by the absorption in the layer of red phosphor. The granules of blue phosphor convert the blue light into green light as the said phosphor absorbs the blue light generated by the chip of LED. Besides the blue light mentioned, the granules of ZnS:Eu²⁺ also absorb the yellow light. Between the said absorptions, because of the substance's absorption features, the absorption of the blue light generated by the chip of LED displays more potency. Therefore, the WLEDs' green element is boosted when ZnS:Eu²⁺ is introduced, which boosts the chromatic homogeneity as a result. Among today's WLED lamp parameters, chromatic uniformity is considered a vital parameter. It is evident that raising the chromatic uniformity can raise the WLED's price. But the use of ZnS:Eu²⁺ can be economical, and as such, it may have widespread application.

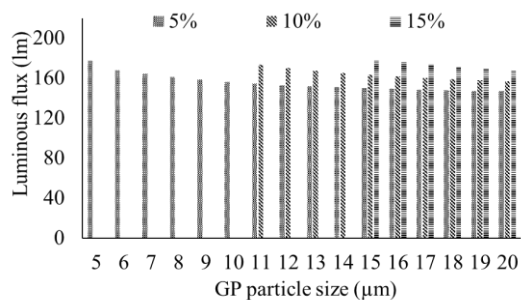


Figure 4. The luminous flux of WLEDs as a function of ZnS:Eu²⁺ concentration

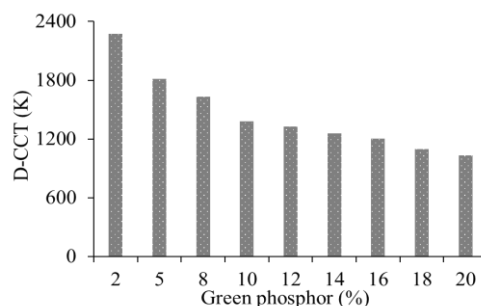


Figure 5. The color deviation of WLEDs as a function of ZnS:Eu²⁺ concentration

When it comes to determining the WLEDs' chromatic performance, chromatic uniformity is the sole aspect. Great chromatic uniformity does not guarantee decent chromatic performance. As such, earlier studies propose a parameter to determine the color generation and chromatic quality. When lights from the tested illumination source are casted on surfaces of targeted objects, the color rendering index takes their genuine color. The lack of chromatic homogeneity is the result of the green-light presence being overabundant among the three main colors, which are blue, yellow and green. Such outcome has an impact on the WLED's chromatic performance, which can harm the chromatic uniformity. When the layer of remote phosphor

ZnS:Eu²⁺ is added, we can see that in Figure 6, CRI decreases by a small amount. However, such drawbacks are insignificant as CRI is merely a CQS's downside. Judging both CRI and CQS, it is more difficult to acquire the CQS and the CQS should be favored over CRI. The CQS parameter takes into account three facets: CRI, beholder's taste, and color coordinate. With such important facets, CQS can be considered the effective and general parameter determining the chromatic performance. With the layer of remote phosphor ZnS:Eu²⁺, the boost in CQS can be seen in Figure 7. Furthermore, as the phosphor ZnS:Eu²⁺ concentration rises, the CQS does not display any remarkable change when the said concentration is below 10% wt. If the concentration exceeds 10% wt., CRI and CQS all suffer from a considerable fall caused by the tremendous loss of color due to the prevalence of green color. As such, we must choose an appropriate concentration of green phosphor ZnS:Eu²⁺.

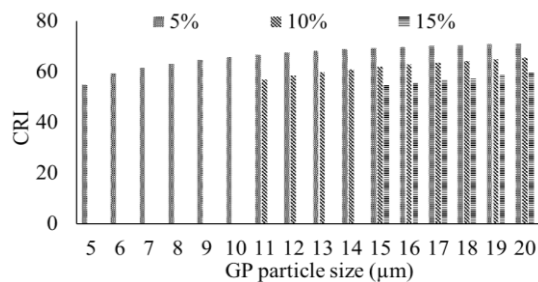


Figure 6. The color rendering index of WLEDs as a function of ZnS:Eu²⁺ concentration

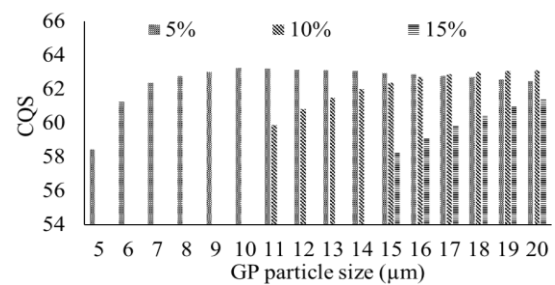


Figure 7. The color quality scale of WLEDs as a function of ZnS:Eu²⁺ concentration

4. CONCLUSION

Our research demonstrates how the green phosphor ZnS:Eu²⁺ can affect the light attributes in the two-layer phosphor package. Through the Monte Carlo recreation on computer, our research confirms that ZnS:Eu²⁺ can be chosen to boost the chromatic homogeneity, which applies to WLEDs at the small color temperature of 5000 K as well as the color temperature over 8500 K. The discovery of the research has, therefore, met its goal of boosting the chromatic performance and lumen, a complex task for the remote phosphor package. But there is a small downside for the CRI and CQS. As the ZnS:Eu²⁺ concentration rises too high, the said parameters go down substantially. As such, we must choose an appropriate concentration, depending on the manufacturer's goals. This article can provide lots of vital data to be used for reference when it comes to producing better chromatic homogeneity and lumen in WLEDs.

ACKNOWLEDGEMENTS

This research is supported by Industrial University of Ho Chi Minh City (IUH) under grant number 121/HD-DHCN.

REFERENCES

- [1] T. De Rubeis, F. Smarra, N. Gentile, A. D'innocenzo, D. Ambrosini, and D. Paoletti, "Learning lighting models for optimal control of lighting system via experimental and numerical approach," *Science and Technology for the Built Environment*, vol. 27, no. 8, pp. 1018–1030, Sep. 2021, doi: 10.1080/23744731.2020.1846427.
- [2] N. Eisazadeh, K. Allacker, and F. De Troyer, "Integrated energy, daylighting and visual comfort analysis of window systems in patient rooms," *Science and Technology for the Built Environment*, vol. 27, no. 8, pp. 1040–1055, Sep. 2021, doi: 10.1080/23744731.2021.1912512.
- [3] J. Zhang, Y. Meuret, X. Wang, and K. A. G. Smet, "Improved and robust spectral reflectance estimation," *Leukos*, vol. 17, no. 4, pp. 359–379, Oct. 2021, doi: 10.1080/15502724.2020.1798246.
- [4] A. M. Salim and S. Abu Dabous, "Quantitative analysis of sustainable housing energy systems based on Estidama pearl rating system," *International Journal of Green Energy*, vol. 15, no. 14–15, pp. 905–917, Dec. 2018, doi: 10.1080/15435075.2018.1529585.
- [5] K. R. Shailesh, "Understanding multi-domain compact modeling of light-emitting diodes," *Cogent Engineering*, vol. 8, no. 1, Jan. 2021, doi: 10.1080/23311916.2021.1915730.
- [6] M. Yazdan Mehr, A. Bahrami, W. D. van Driel, X. J. Fan, J. L. Davis, and G. Q. Zhang, "Degradation of optical materials in solid-state lighting systems," *International Materials Reviews*, vol. 65, no. 2, pp. 102–128, Feb. 2020, doi: 10.1080/09506608.2019.1565716.
- [7] A. Dawodu, A. Cheshmehzangi, and A. Sharifi, "A multi-dimensional energy-based analysis of neighbourhood sustainability assessment tools: are institutional indicators really missing?," *Building Research and Information*, vol. 49, no. 5, pp. 574–592,

- Jul. 2021, doi: 10.1080/09613218.2020.1806701.
- [8] L. Ferro Desideri, F. Barra, S. Ferrero, C. E. Traverso, and M. Nicolò, "Clinical efficacy and safety of ranibizumab in the treatment of wet age-related macular degeneration," *Expert Opinion on Biological Therapy*, vol. 19, no. 8, pp. 735–751, Aug. 2019, doi: 10.1080/14712598.2019.1627322.
- [9] S. J. Roberts, J. R. Rudd, and M. J. Reeves, "Efficacy of using non-linear pedagogy to support attacking players' individual learning objectives in elite-youth football: A randomised cross-over trial," *Journal of Sports Sciences*, vol. 38, no. 11–12, pp. 1454–1464, Jun. 2020, doi: 10.1080/02640414.2019.1609894.
- [10] G. Wang, S.-C. Hwang, W.-H. Kim, and G.-S. Kil, "Design and fabrication of an LED lantern based on light condensing technology," *Journal of International Council on Electrical Engineering*, vol. 8, no. 1, pp. 14–18, Jan. 2018, doi: 10.1080/22348972.2018.1436894.
- [11] O. H. Kwon, J. S. Kim, J. W. Jang, and Y. S. Cho, "Simple prismatic patterning approach for nearly room-temperature processed planar remote phosphor layers for enhanced white luminescence efficiency," *Optical Materials Express*, vol. 8, no. 10, pp. 3230–3237, Oct. 2018, doi: 10.1364/OME.8.003230.
- [12] X. Leng *et al.*, "Feasibility of co-registered ultrasound and acoustic-resolution photoacoustic imaging of human colorectal cancer," *Biomedical Optics Express*, vol. 9, no. 11, pp. 5159–5172, Nov. 2018, doi: 10.1364/BOE.9.005159.
- [13] D. Molter, M. Kolano, and G. von Freymann, "Terahertz cross-correlation spectroscopy driven by incoherent light from a superluminescent diode," *Optics Express*, vol. 27, no. 9, pp. 12659–12665, Apr. 2019, doi: 10.1364/OE.27.012659.
- [14] A. Ali *et al.*, "Blue-laser-diode-based high CRI lighting and high-speed visible light communication using narrowband green/red-emitting composite phosphor film," *Applied Optics*, vol. 59, no. 17, pp. 5197–5204, Jun. 2020, doi: 10.1364/AO.392340.
- [15] S. Beldi *et al.*, "High Q-factor near infrared and visible Al₂O₃-based parallel-plate capacitor kinetic inductance detectors," *Optics Express*, vol. 27, no. 9, pp. 13319–13328, Apr. 2019, doi: 10.1364/OE.27.013319.
- [16] C.-H. Lin *et al.*, "Hybrid-type white LEDs based on inorganic halide perovskite QDs: candidates for wide color gamut display backlights," *Photonics Research*, vol. 7, no. 5, pp. 579–585, May 2019, doi: 10.1364/PRJ.7.000579.
- [17] W.-Y. Chang, Y. Kuo, Y.-W. Kiang, and C. C. Yang, "Simulation study on light color conversion enhancement through surface plasmon coupling," *Optics Express*, vol. 27, no. 12, pp. A629–A642, Jun. 2019, doi: 10.1364/OE.27.00A629.
- [18] X. Xi *et al.*, "Chip-level Ce:GdYAG ceramic phosphors with excellent chromaticity parameters for high-brightness white LED device," *Optics Express*, vol. 29, no. 8, pp. 11938–11946, Apr. 2021, doi: 10.1364/OE.416486.
- [19] L. Xiao, C. Zhang, P. Zhong, and G. He, "Spectral optimization of phosphor-coated white LED for road lighting based on the mesopic limited luminous efficacy and IES color fidelity index," *Applied Optics*, vol. 57, no. 4, Feb. 2018, doi: 10.1364/AO.57.000931.
- [20] H.-P. Huang, M. Wei, and L.-C. Ou, "White appearance of a tablet display under different ambient lighting conditions," *Optics Express*, vol. 26, no. 4, pp. 5018–5030, Feb. 2018, doi: 10.1364/OE.26.005018.
- [21] L. Duan and Z. Lei, "Wide color gamut display with white and emerald backlighting," *Applied Optics*, vol. 57, no. 6, pp. 1338–1344, Feb. 2018, doi: 10.1364/AO.57.001338.
- [22] H. Ando and S. Ryu, "Simultaneous dual data stream transmission using RGB and phosphor-based white LEDs," in *2018 Asia Communications and Photonics Conference (ACP)*, Oct. 2018, pp. 1–3, doi: 10.1109/ACP.2018.8596012.
- [23] H. Liu, Y. Shi, and T. Wang, "Design of a six-gas NDIR gas sensor using an integrated optical gas chamber," *Optics Express*, vol. 28, no. 8, pp. 11451–11462, Apr. 2020, doi: 10.1364/OE.388713.
- [24] T. Y. Orudzhev, S. G. Abdullaeva, and R. B. Dzhabbarov, "Increasing the extraction efficiency of a light-emitting diode using a pyramid-like phosphor layer," *Journal of Optical Technology*, vol. 86, no. 10, pp. 671–676, Oct. 2019, doi: 10.1364/JOT.86.000671.
- [25] P. Kumar and N. K. Nishchal, "Enhanced exclusive-OR and quick response code-based image encryption through incoherent illumination," *Applied Optics*, vol. 58, no. 6, pp. 1408–1412, Feb. 2019, doi: 10.1364/AO.58.001408.

BIOGRAPHIES OF AUTHORS



Dieu An Nguyen Thi    received a master of Electrical Engineering, HCMC University of Technology and Education, Viet Nam. Currently, she is a lecturer at the Faculty of Electrical Engineering Technology, Industrial University of Ho Chi Minh City, Viet Nam. Her research interests are Theoretical Physics and Mathematical Physics. She can be contacted at email: nguyenthidieuan@iuh.edu.vn.



Phuc Dang Huu    received a Physics Ph.D. degree from the University of Science, Ho Chi Minh City, in 2018. Currently, He is Research Institute of Applied Technology, Thu Dau Mot University, Binh Duong Province, Vietnam. His research interests include simulation LEDs material, renewable energy. He can be contacted at email: danghuuphuc@tdmu.edu.vn.